Electronic Supplementary Material (ESI) for New Journal of Chemistry.

Synthesis and photophysical properties of rare earths (La, Nd, Gd, Y, Ho) complexes with silanediamido ligands bearing chelating phenylbenzothiazole chromophore

Olga A. Mironova*, Aleksey A. Ryadun, Taisiya S. Sukhikh, Nikolay A. Pushkarevsky, Sergey N. Konchenko

* Corresponding author at Nikolaev Institute of Inorganic Chemistry SB RAS, Akademika Lavrentieva Ave. 3, 630090 Novosibirsk, Russia. E-mail: mironova@niic.nsc.ru (O.A. Mironova)

Table of contents:

1. Reactions of H_2L with KH in presence of $LnCl_3$

For **2**^{La}: 55 mg (0.22 mmol) of $LaCl_3$, 227 mg (0.446 mmol) of H_2L, and 36 mg (0.90 mmol) of KH were placed in a Schlenk tube, and 5 mL of thf were condensed. The reaction mixture was stirred at 70 °C for 3 days with periodical degassing, during which the solution turned red. Precipitated KCl was centrifuged off, the solution was placed into a bent two-section ampoule, and 3 mL of hexane were added. The ampoule was evacuated and sealed, the solvent was fully transferred to the second section, and soluble products were extracted from the solid residue by placing the ampoule in a temperature gradient of 45 °C – room temperature. Upon concentration of the extract, the complex [{K(thf)$_5$}{LaL$_2$}]crystallized in the form of plates. To obtain a pure powder, crystals were washed two times with hexane and dried. According to NMR, only two thf molecules remain giving the formula [{K(thf)$_2$}{LaL$_2$}]. Yield 254 mg (85%). For $C_{64}H_{60}KLaN_8O_2S_4Si_2$ (1335.65): calcd. C 57.55, H 4.53, N 8.39 %; found C 53.9, H 3.8, N 8.1%. The elemental analysis results evidence either the incomplete conversion to the desired bis-ligand complex or the contamination with inorganic impurity (KCl).

For **2**^{Gd}: the compound was synthesized analogously to the previous one, starting from 57 mg (0.22 mmol) of $GdCl_3$, 220 mg (0.432 mmol) of H_2L, and 37 mg (0.93 mmol) of KH. The compound crystallizes as red plates of [{K(thf)$_6$}{GdL$_2$}]. Yield 152 mg (52 %, considering the compound in solid phase to have the same formula as **2**^{La}, [{K(thf)$_2$}{GdL$_2$}]).For $C_{64}H_{60}KGdN_8O_2S_4Si_2$ (1354.00): calcd. C 56.77, H 4.47, N 8.28 %; found C 53.1, H 4.0, N 7.8 %. The elemental analysis results evidence either the incomplete conversion to the desired bis-ligand complex or the contamination with inorganic impurity (KCl).

2. X-ray structural determination

Table S1. Crystal data and structure refinement for the compounds.

Identification code	**1^{H}**	**1^{Li}**	**Li(NH-pbt)**	**2^{La}**	**2^{Gd}**·THF	**3^{Y}**·2THF	**3^{La}**·C_7H_8	**3Nd**·2THF	**4^{Ho}**·0.5C_7H_8
CCDC number	2217650	2217651	2217648	2217655	2217656	2217653	2217652	2217654	2217649
Empirical formula	$C_{28}H_{24}N_4S_2Si$	$C_{44}H_{54}Li_2N_4O_4S_2Si$	$C_{34}H_{34}Li_2N_4O_2S_2$	$C_{76}H_{84}KLaN_8O_5S_4Si_2$	$C_{84}H_{100}GdKN_8O_7S_4Si_2$	$C_{80}H_{92}LiN_8O_6S_4Si_2Y$	$C_{79}H_{84}LaLiN_8O_4S_4Si_2$	$C_{80}H_{92}LiN_8NdO_6S_4Si_2$	$C_{39.5}H_{42}Cl_2HoLiN_4O_2S_2Si$
Formula weight	508.72	809.00	608.65	1551.94	1714.48	1541.88	1539.81	1597.21	939.75
Space group	*C*2/*c*	$P2_12_12_1$	*Pccn*	$P2_1$/c	*P*–1	*Pbcn*	$P2_1$/c	*Pbcn*	$P2_1$/n
a/Å	24.4530(9)	14.2687(5)	22.3632(16)	16.0298(9)	12.3738(3)	19.5493(7)	16.5473(11)	19.8134(8)	8.7223(5)
b/Å	11.5979(5)	23.7559(9)	7.4787(6)	17.5784(11)	18.5982(4)	22.5030(7)	21.5497(13)	22.6439(8)	39.088(2)
c/Å	19.0911(8)	25.5065(10)	18.6220(15)	26.4091(16)	18.9764(5)	17.3269(6)	20.7855(15)	17.0123(5)	11.8281(6)
α/°	90	90	90	90	90.2130(10)	90	90	90	90
β/°	112.782(2)	90	90	96.461(2)	91.5590(10)	90	96.833(2)	90	92.411(2)
γ/°	90	90	90	90	108.2600(10)	90	90	90	90
Volume/Å^3	4991.9(4)	8645.8(6)	3114.5(4)	7394.2(8)	4145.26(17)	7622.4(4)	7359.2(8)	7632.6(5)	4029.1(4)
Z	8	8	4	4	2	4	4	4	4
ρ_{calc}g/cm^3	1.354	1.243	1.298	1.394	1.374	1.344	1.390	1.390	1.549
μ/mm^{-1}	0.287	0.197	0.209	0.835	1.038	0.964	0.783	0.879	2.269
F(000)	2128.0	3440.0	1280.0	3216.0	1782.0	3240.0	3192.0	3324.0	1892.0
Radiation	MoKα (λ = 0.71073)	MoKα (λ = 0.71073)	MoKα (λ = 0.71073)	MoKα (λ = 0.71073)	MoKα (λ = 0.71073)	MoKα (λ = 0.71073)	MoKα (λ = 0.71073)	MoKα (λ = 0.71073)	MoKα (λ = 0.71073)
2Θ range for data collection/°	4.64 to 52.798	3.27 to 51.37	4.738 to 57.396	3.794 to 59.212	4.132 to 54.206	4.316 to 51.412	4.52 to 48.814	4.786 to 55.782	4.654 to 50.202
Index ranges	-24 ≤ h ≤ 30, -11 ≤ k ≤ 14, -23 ≤ l ≤ 20	-17 ≤ h ≤ 17, -26 ≤ k ≤ 28, -31 ≤ l ≤ 31	-28 ≤ h ≤ 30, -10 ≤ k ≤ 8, -22 ≤ l ≤ 25	-22 ≤ h ≤ 21, -23 ≤ k ≤ 24, -34 ≤ l ≤ 36	-15 ≤ h ≤ 15, -23 ≤ k ≤ 22, -24 ≤ l ≤ 24	-23 ≤ h ≤ 23, -27 ≤ k ≤ 27, -21 ≤ l ≤ 21	-19 ≤ h ≤ 18, -25 ≤ k ≤ 24, -24 ≤ l ≤ 20	-26 ≤ h ≤ 18, -29 ≤ k ≤ 21, -19 ≤ l ≤ 22	-10 ≤ h ≤ 10, -46 ≤ k ≤ 46, -14 ≤ l ≤ 13
Reflections collected	24874	90962	19046	99343	50322	136604	41488	59267	34357
Rint, Rsigma	0.0434, 0.0387	0.0726, 0.0595	0.0497, 0.0389	0.0485, 0.0397	0.0599, 0.0755	0.1252, 0.0442	0.0753, 0.0811	0.0602, 0.0403	0.0865, 0.0683
Data/restraints/parameters	5102/2/324	16400/48/1042	4011/1/202	20204/198/970	18167/176/1064	7246/11/468	12080/23/879	9096/12/468	7143/109/512
Goodness-of-fit on F^2	1.170	1.031	1.044	1.021	1.022	1.017	1.019	1.028	1.016
Final R indexes [I>=2σ (I)]	R_1 = 0.0543, wR_2 = 0.1079	R_1 = 0.0527, wR_2 = 0.1314	R_1 = 0.0390, wR_2 = 0.0944	R_1 = 0.0311, wR_2 = 0.0685	R_1 = 0.0465, wR_2 = 0.0917	R_1 = 0.0423, wR_2 = 0.0980	R_1 = 0.0443, wR_2 = 0.0837	R_1 = 0.0369, wR_2 = 0.0835	R_1 = 0.0448, wR_2 = 0.0816
Final R indexes [all data]	R_1 = 0.0645, wR_2 = 0.1118	R_1 = 0.0718, wR_2 = 0.1474	R_1 = 0.0501, wR_2 = 0.1009	R_1 = 0.0411, wR_2 = 0.0742	R_1 = 0.0626, wR_2 = 0.1008	R_1 = 0.0731, wR_2 = 0.1155	R_1 = 0.0737, wR_2 = 0.0952	R_1 = 0.0556, wR_2 = 0.0952	R_1 = 0.0661, wR_2 = 0.0892
Largest diff. peak/hole / e Å^{-3}	0.39/-0.27	0.38/-0.38	0.26/-0.23	0.55/-0.42	1.06/-0.94	0.44/-0.48	0.58/-0.54	0.61/-0.55	0.78/-0.78
Flack parameter		0.37(12)							

3. NMR and IR spectroscopy

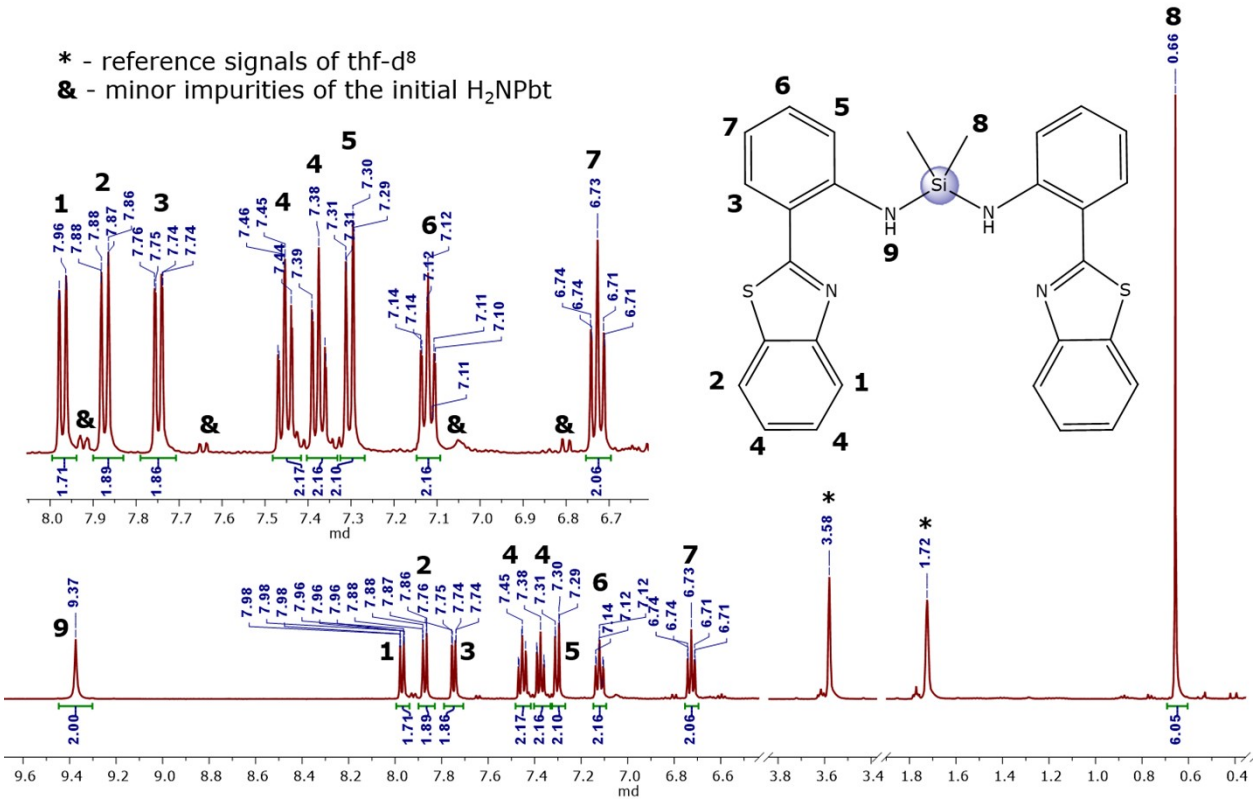

Figure S1. ^{1}H NMR spectrum of $\mathbf{1^{H}}$ in thf-d_8.

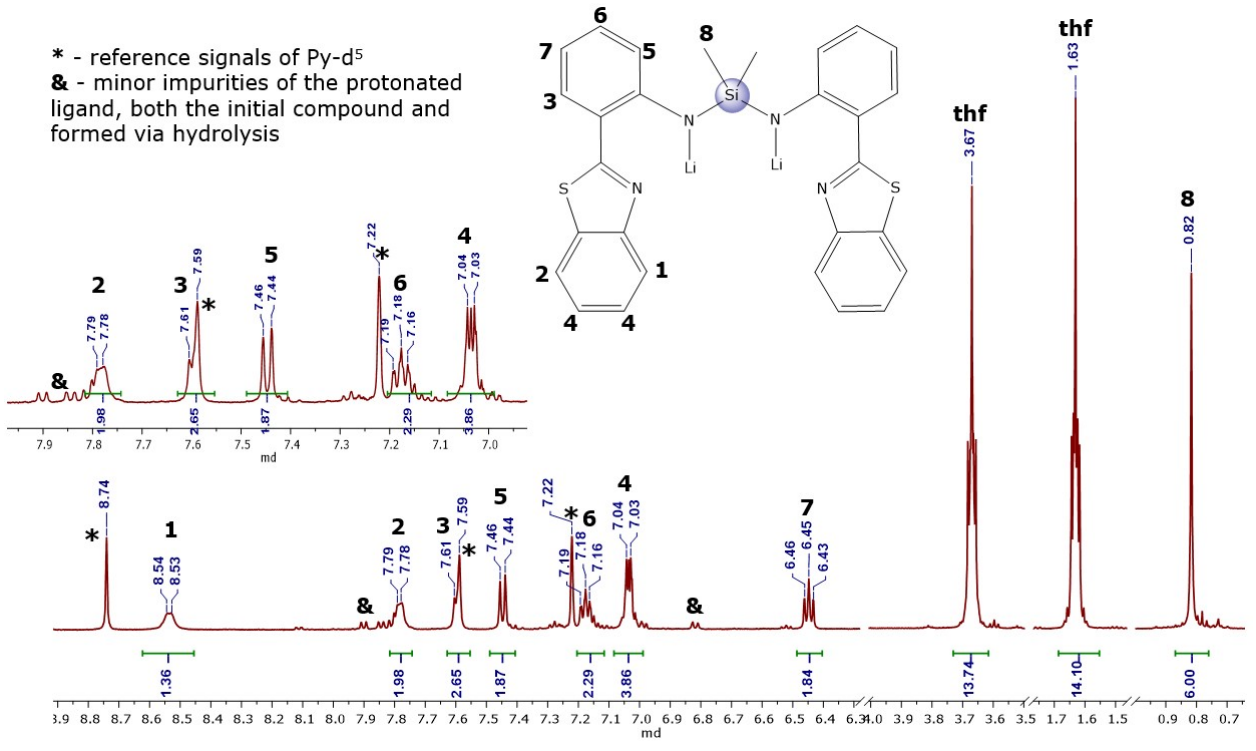

Figure S2. ^{1}H NMR spectrum of $\mathbf{1^{Li}}$ in pyridine-d_5.

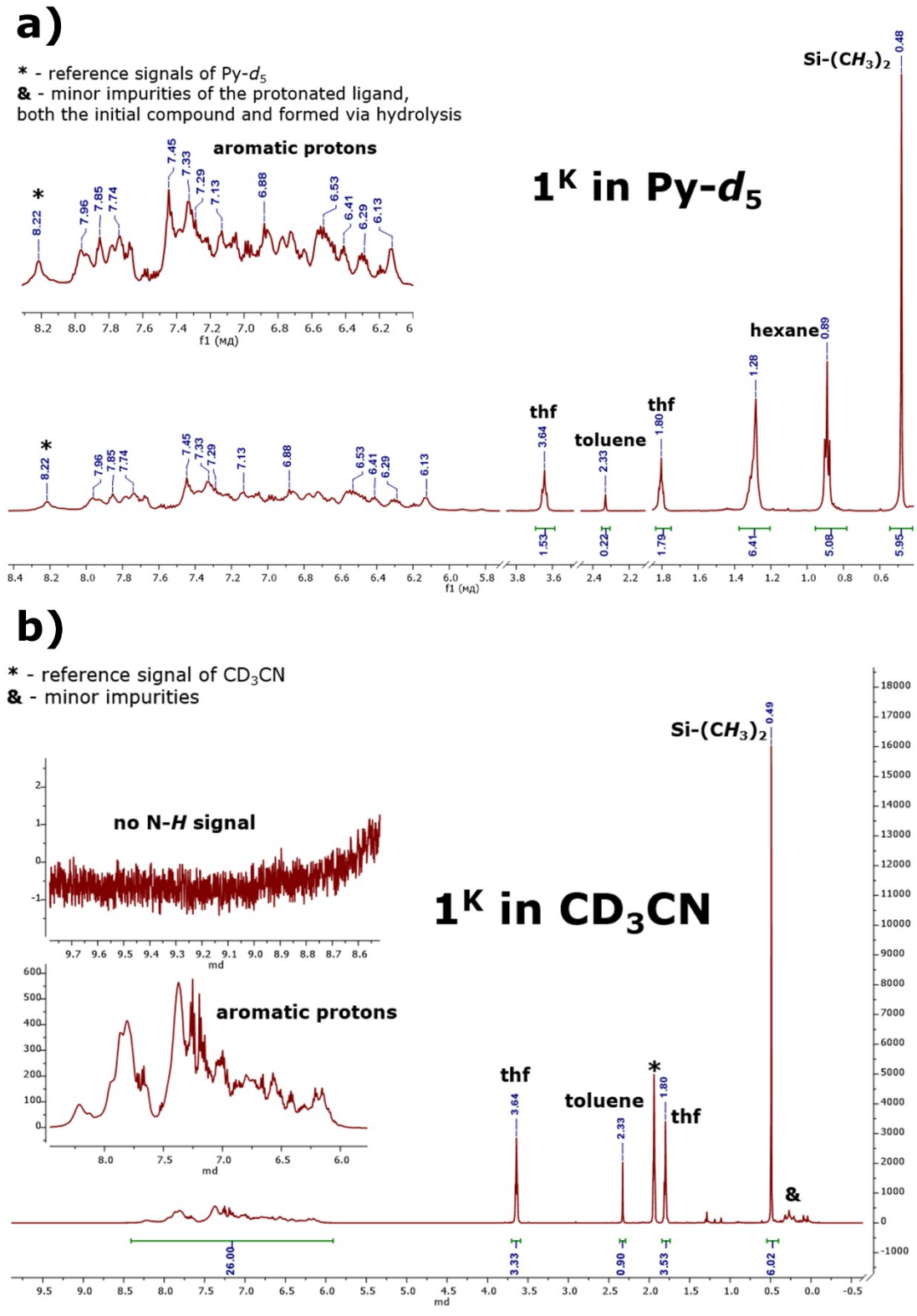

Figure S3. ^{1}H NMR spectra of **1^K** ***a)*** washed with hexane sample in pyridine-d_5; ***b)*** in CD_3CN.

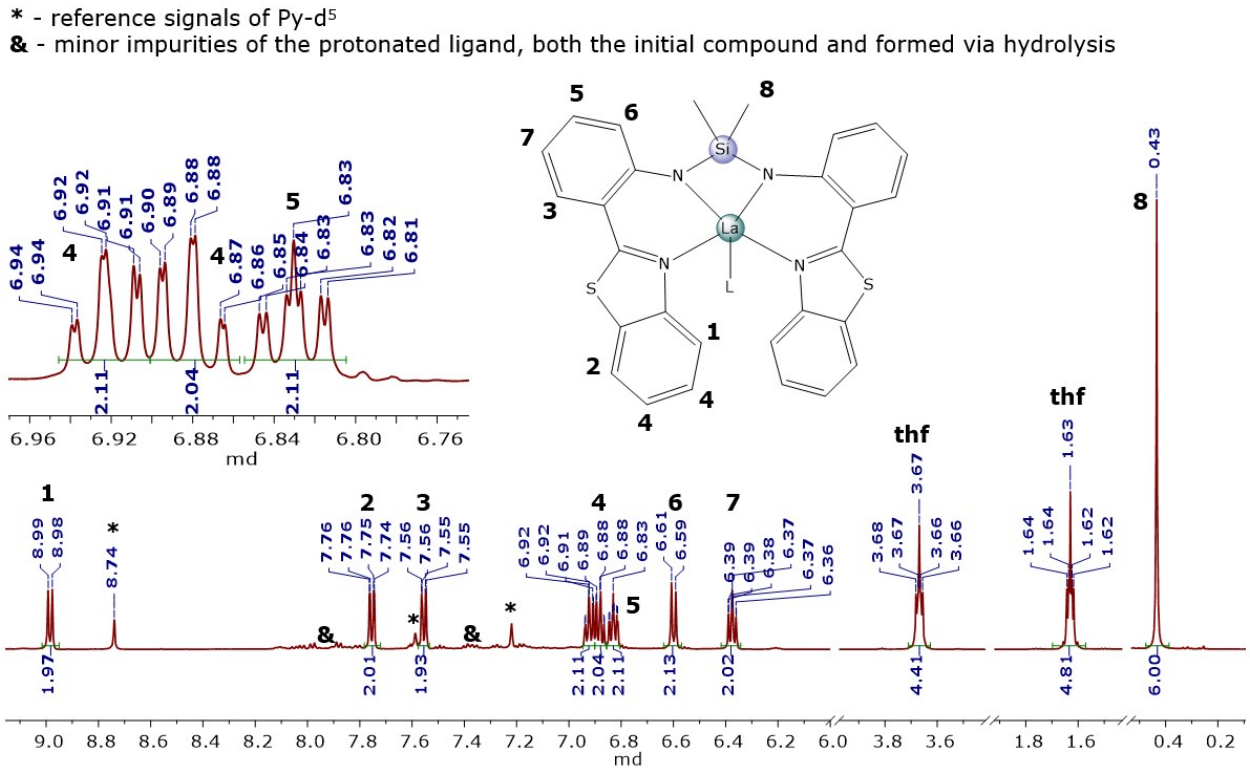

Figure S4. ^{1}H NMR spectrum of **2^{La}** in pyridine-d_5.

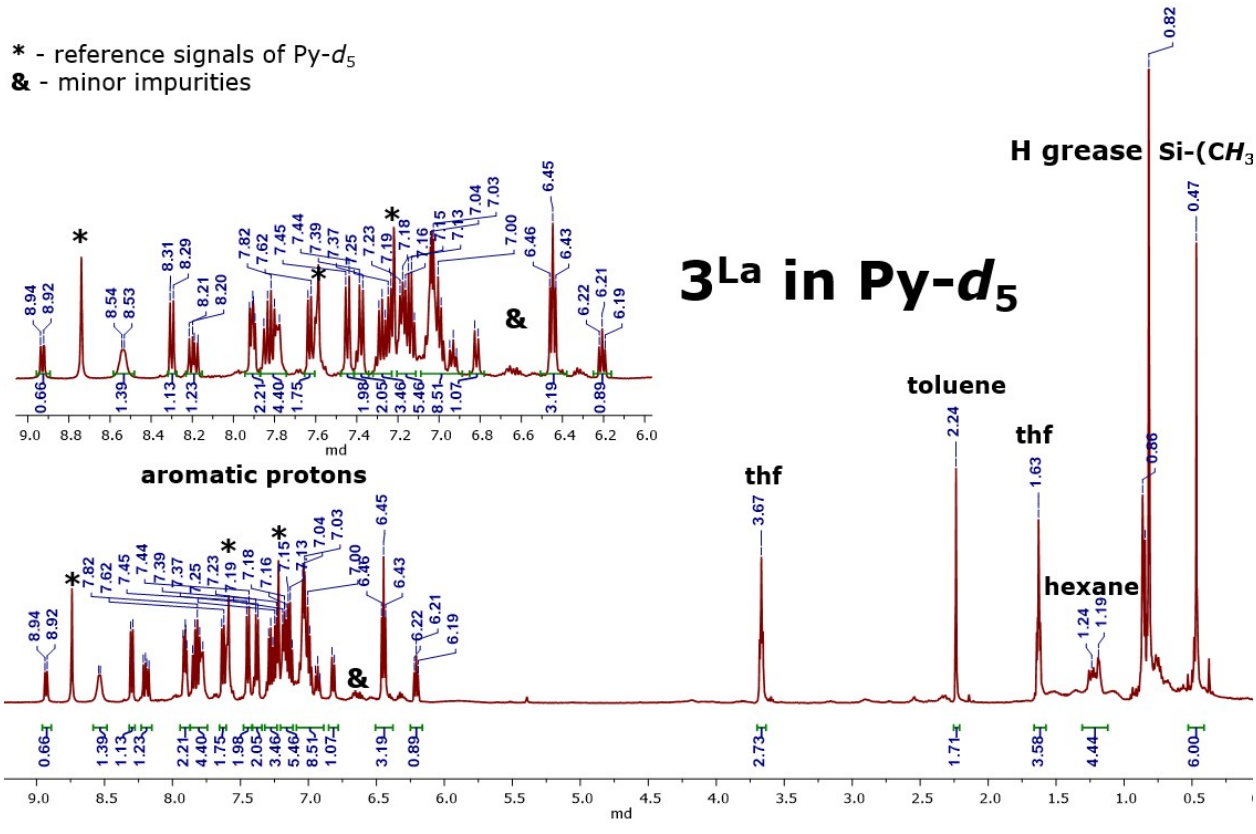

Figure S5. ^{1}H NMR spectrum of **3^{La}** in pyridine-d_5.

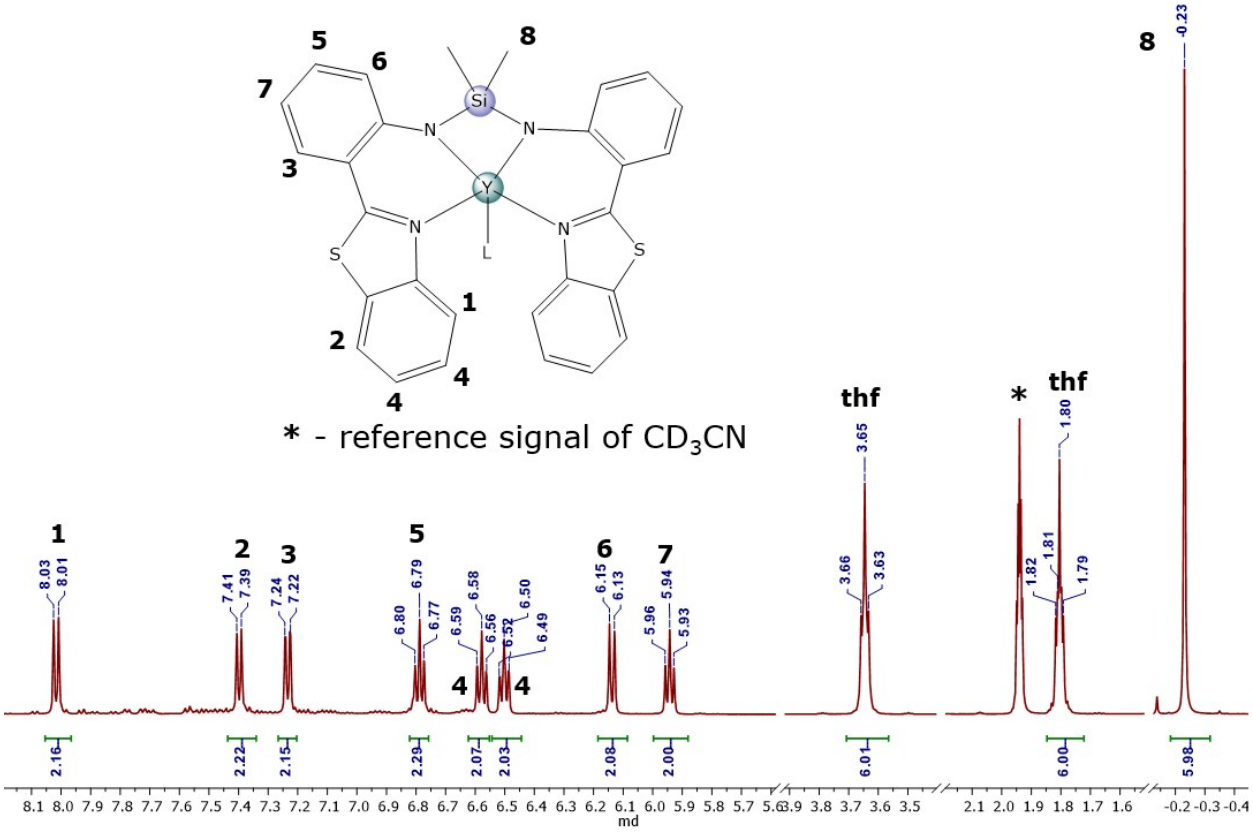

Figure S6. ^{1}H NMR spectrum of **3^{Y}** in CD_3CN.

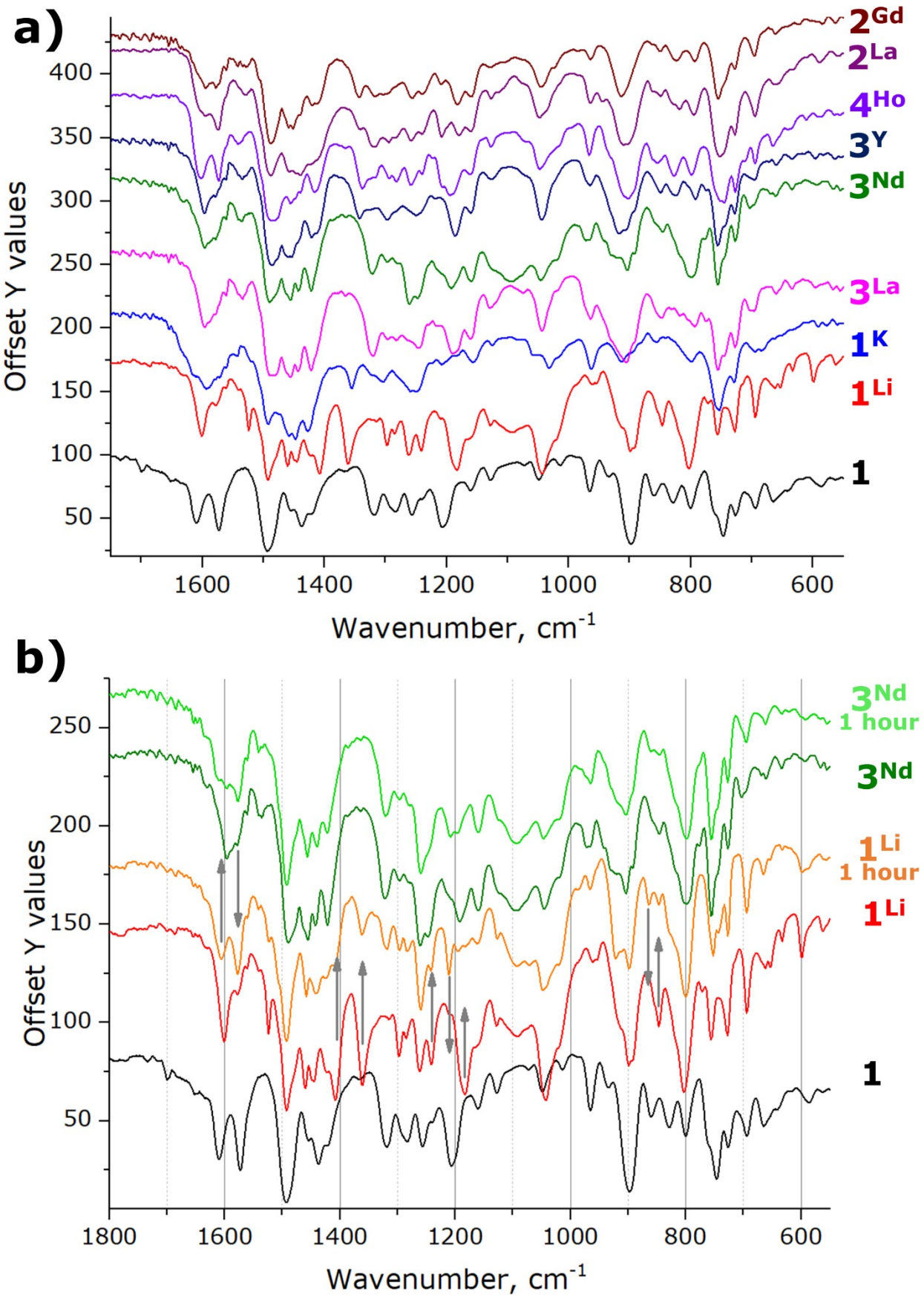

Figure S7. ***a)*** IR spectra of compounds; ***b)*** degradation in the air with time. Arrows point to the changes in the pattern.

4. Electronic absorption spectra

Table S2. Absorption maxima and molar extinction coefficients of $\mathbf{1}^{H}$, $\mathbf{1}^{Li}$, $\mathbf{1}^{K}$, $\mathbf{2}^{La}$, $\mathbf{2}^{Gd}$, $\mathbf{3}^{Nd}$ and $\mathbf{4}^{Ho}$ in thf solutions, and of $\mathbf{4}^{Ho}$ in benzene solution.

Compound	λ, nm	ε, 10^{-4} $M^{-1}cm^{-1}$	Compound	λ, nm	ε, 10^{-4} $M^{-1}cm^{-1}$
$\mathbf{1}^{H}$	252	2.62	$\mathbf{1}^{K}$	250	4.18
	259	2.37		275	3.58
	282	1.93		291 *(sh)*	3.13
	293	2.24		306	2.49
	306	1.52		317 *(sh)*	1.96
	368 *(br)*	2.33		380 *(br)*	1.07
				450 *(br)*	1.44
				500 *(br, sh)*	0.72
$\mathbf{1}^{Li}$	264	4.23	$\mathbf{3}^{Nd}$	272	3.54
	281	3.65		294	2.77
	293	3.39		305 *(sh)*	2.29
	308	2.46		316 *(sh)*	1.70
	382 *(br)*	1.88		384 *(br)*	0.76
	461 *(br)*	1.63		464 *(br)*	1.64
$\mathbf{2}^{La}$	254	6.41	$\mathbf{2}^{Gd}$	253	6.84
	262	6.33		260	6.73
	281	6.49		282	6.58
	291	6.20		290	6.34
	374 *(br)*	2.89		373 *(br)*	3.27
	447 *(br)*	2.21		442 *(br)*	2.22
	498 *(br, sh)*	1.43		498 *(br, sh)*	1.31
$\mathbf{4}^{Ho}$ (thf, $1.2\cdot10^{-3}$ M)	281	2.74	$\mathbf{4}^{Ho}$ (benzene, $6.1\cdot10^{-4}$ M)	283	2.43
	293	2.90		293	2.47
	306	2.18		305	1.84
	370 *(br)*	2.37		372 *(br)*	1.73
	447 *(br)*	0.53		432 *(br)*	0.50

(br) Broad bands are marked

(sh) The band appears as a shoulder to a more intensive band

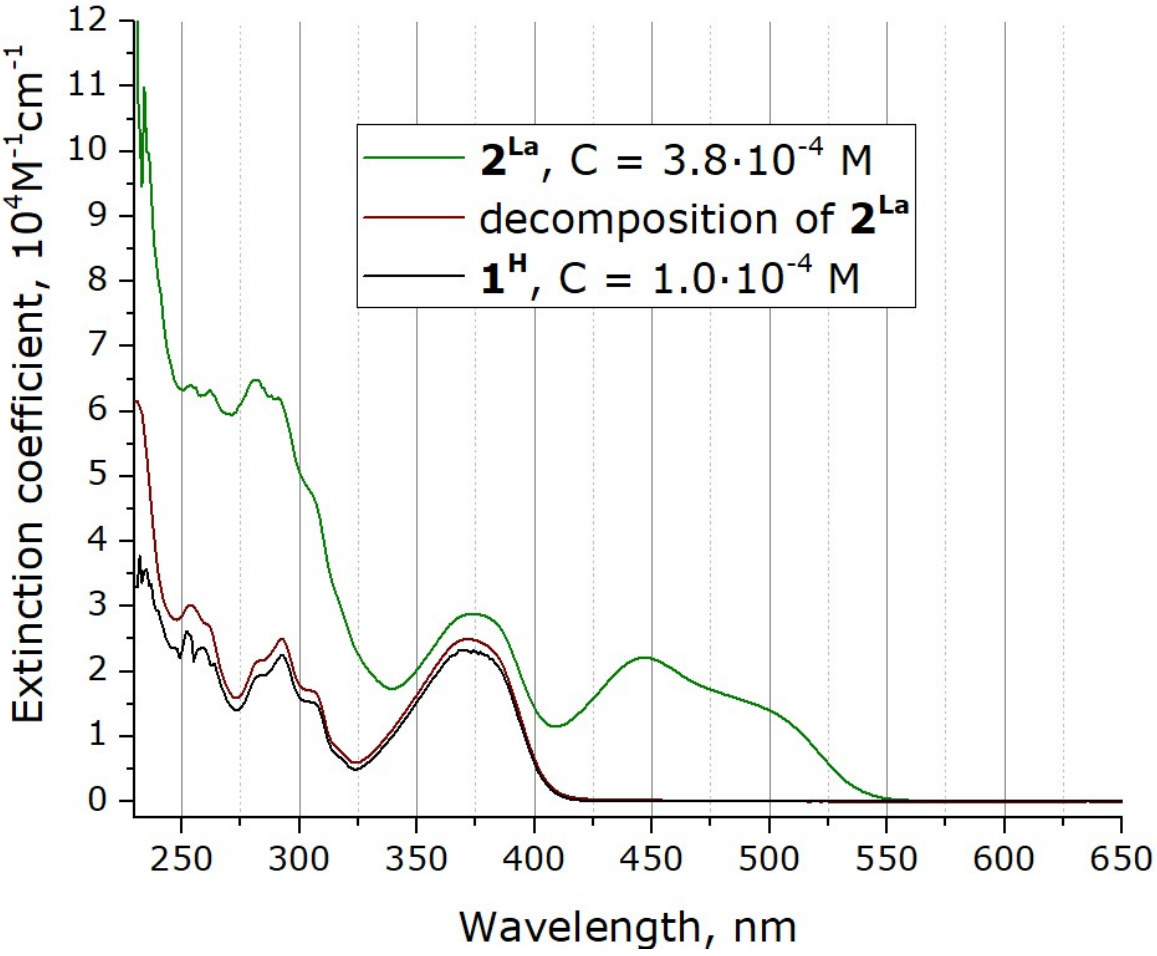

Figure S8. Electronic absorption spectra of $\mathbf{2}^{La}$ upon decomposition and **1** in thf.

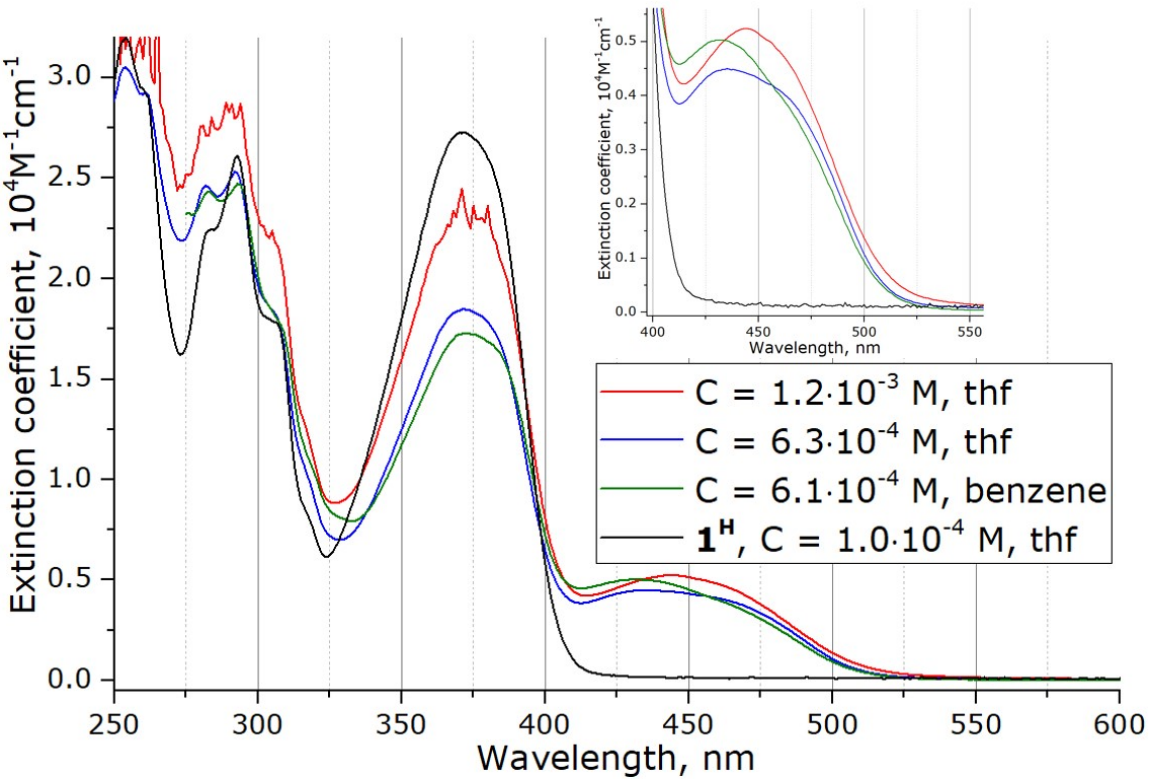

Figure S9. Electronic absorption spectra of $\mathbf{4}^{Ho}$ (colored) and $\mathbf{1}^{H}$ in thf.

5. Excitation and emission spectra

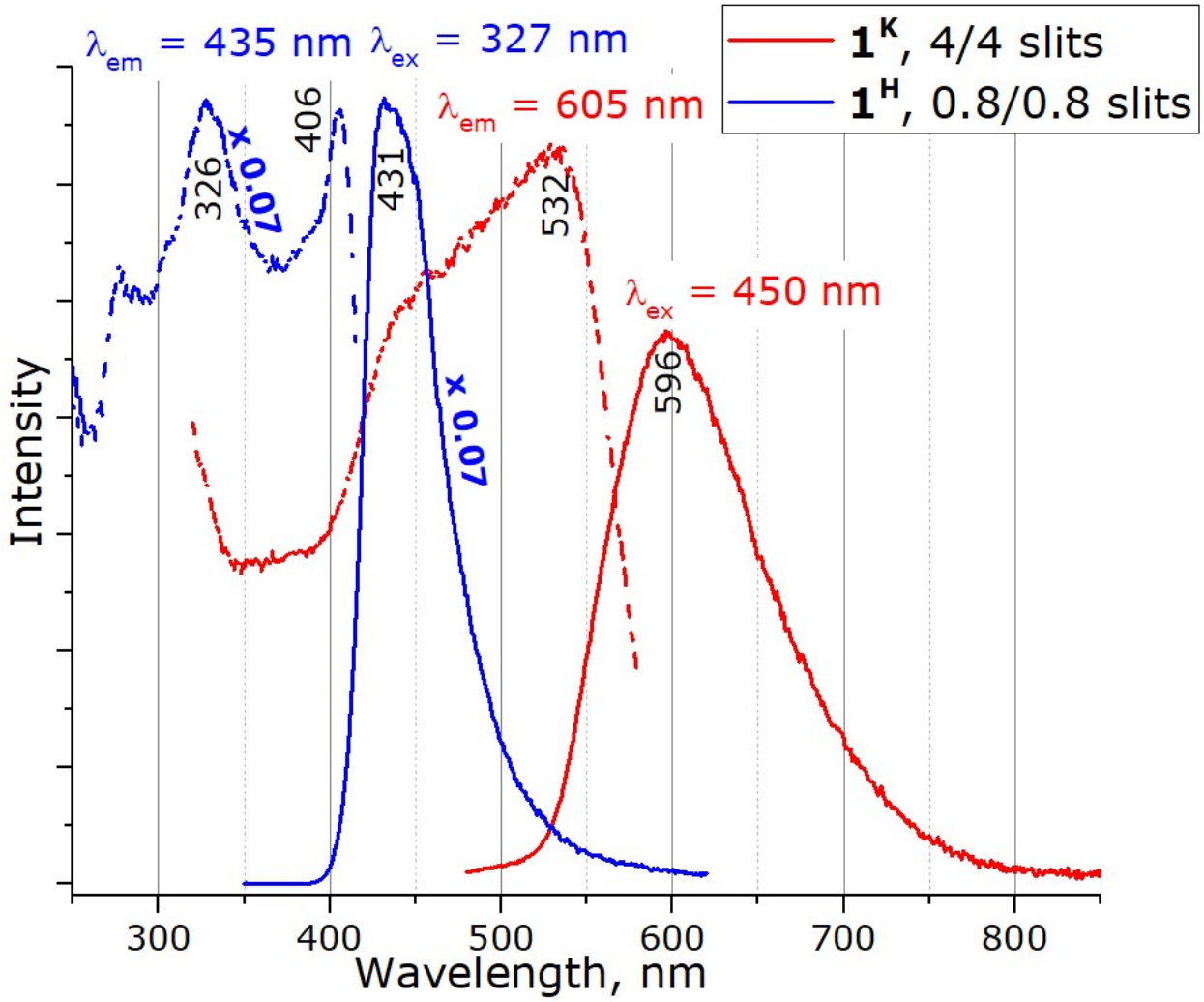

Figure S10. Comparison of $\mathbf{1}^{H}$ and $\mathbf{1}^{K}$ spectra of crystalline samples. The excitation plots are shown with dashed lines, the emission plots are shown with solid lines.

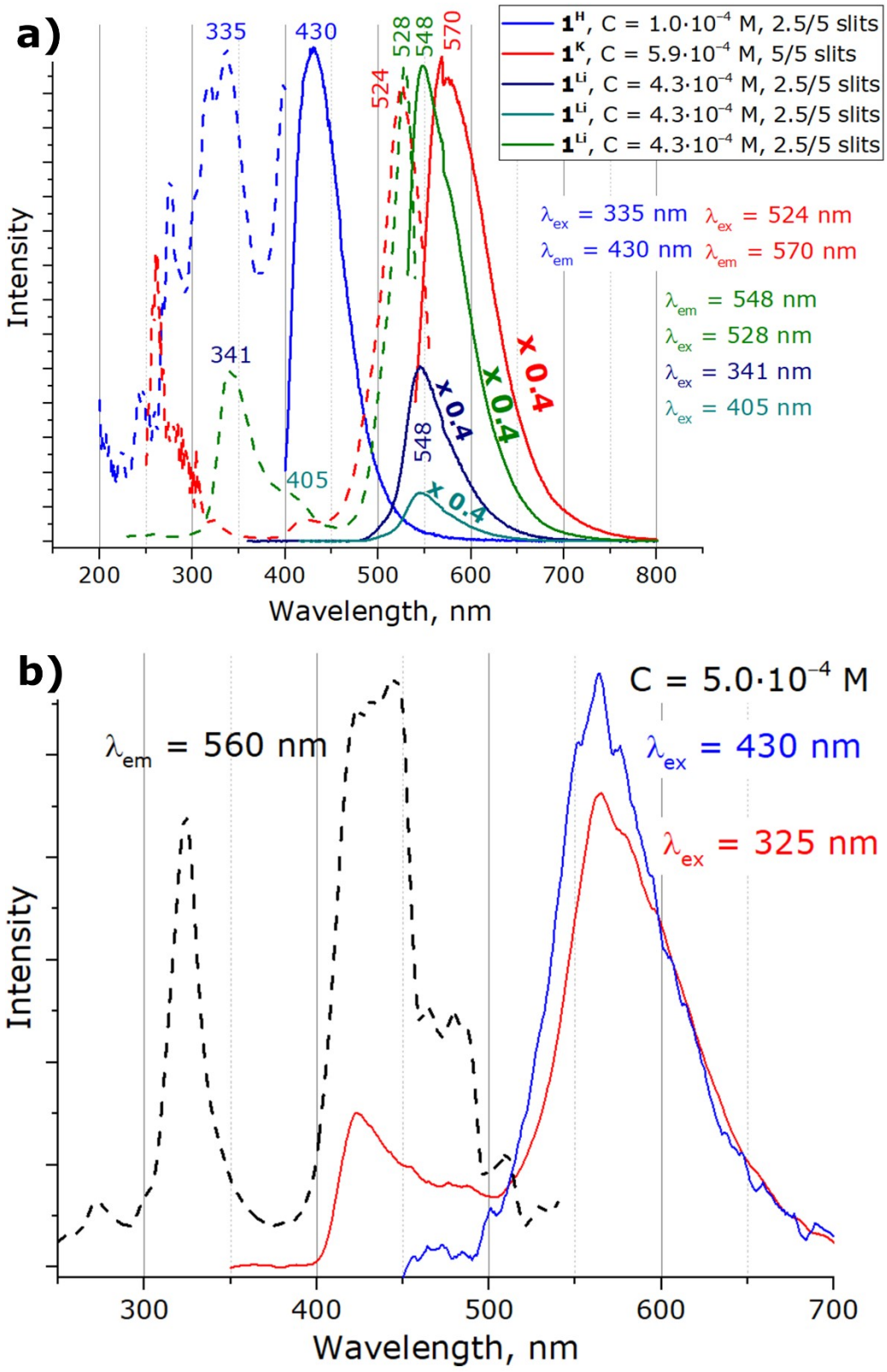

Figure S11. ***a)*** $\mathbf{1}^{H}$, $\mathbf{1}^{Li}$ and $\mathbf{1}^{K}$ spectra in thf solution; ***b)*** partially decomposed sample of $\mathbf{1}^{K}$ in thf solution. The excitation plots are shown with dashed lines, the emission plots are shown with solid lines.

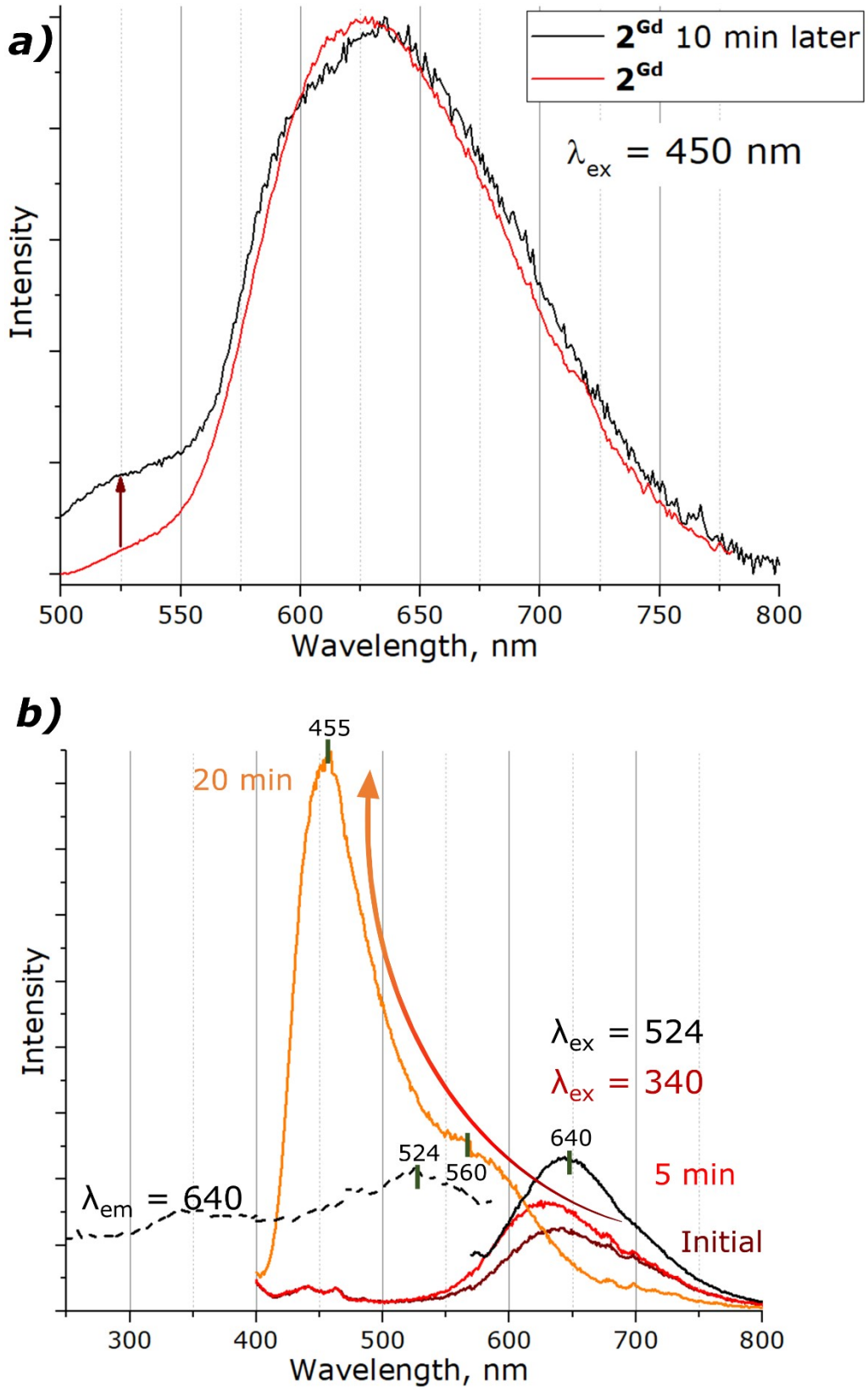

Figure S12. Gradual decomposition of the **2**^{Gd} sample ***a)*** crystalline; ***b)*** in thf solution (C = $4.1 \cdot 10^{-4}$ M). The excitation plot is shown with a dashed line, the emission plots are shown with solid lines.

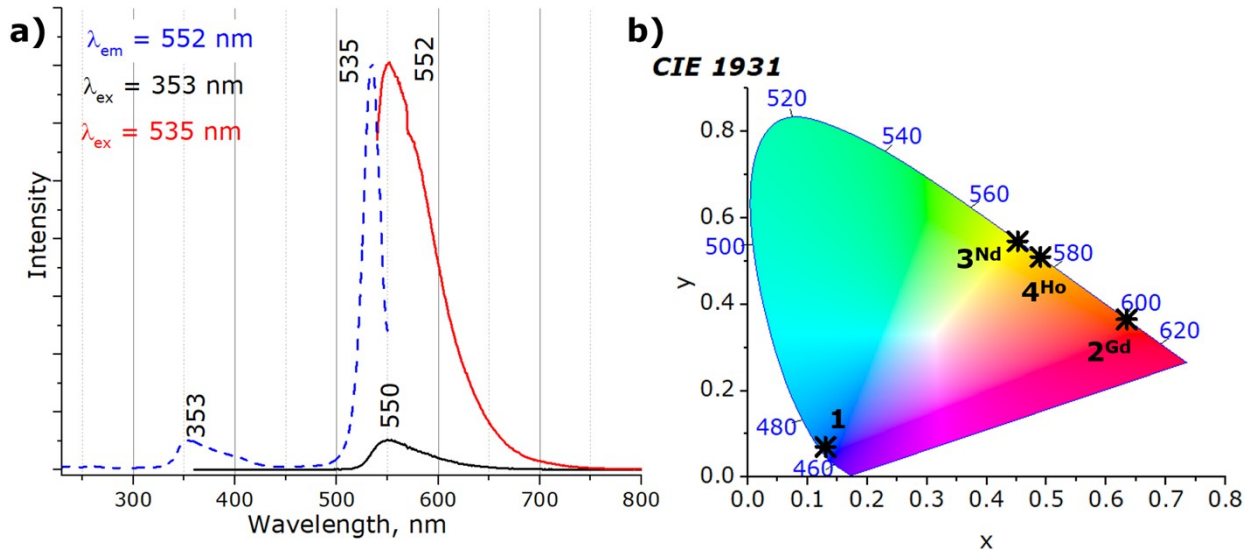

Figure S13. ***a)*** Intraligand emission of $\mathbf{3^{Nd}}$ complex in thf solution (C = $5.0 \cdot 10^{-4}$ M); ***b)*** chromaticity diagram of **1**, $\mathbf{2^{Gd}}$, $\mathbf{3^{Nd}}$, $\mathbf{4^{Ho}}$ emissions in thf solutions. The excitation plot is shown with a dashed line, the emission plots are shown with solid lines.

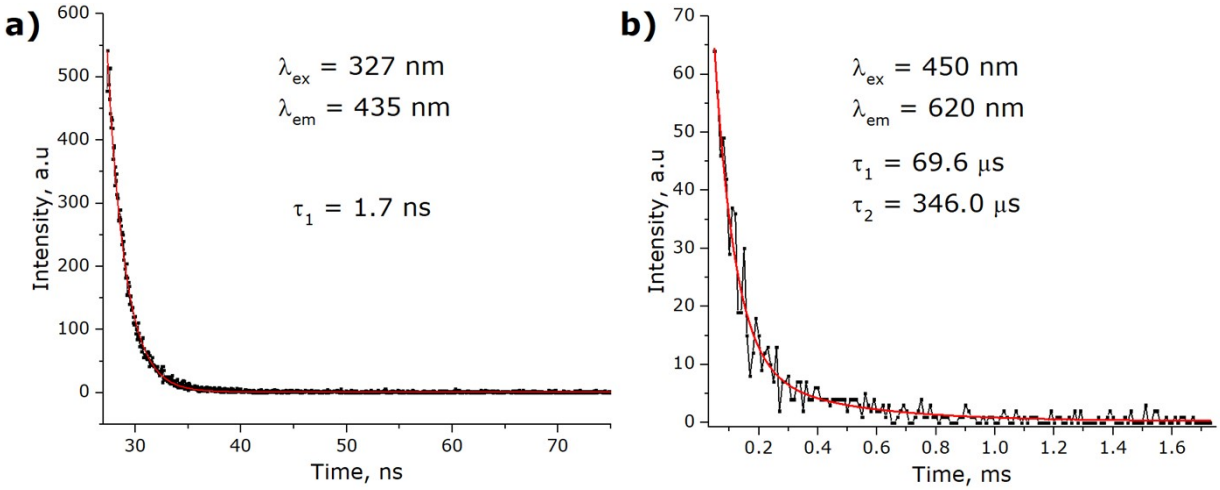

Figure S14. Emission decay curves of solid samples of ***a)*** H_2L; ***b)*** $\mathbf{2^{Gd}}$.

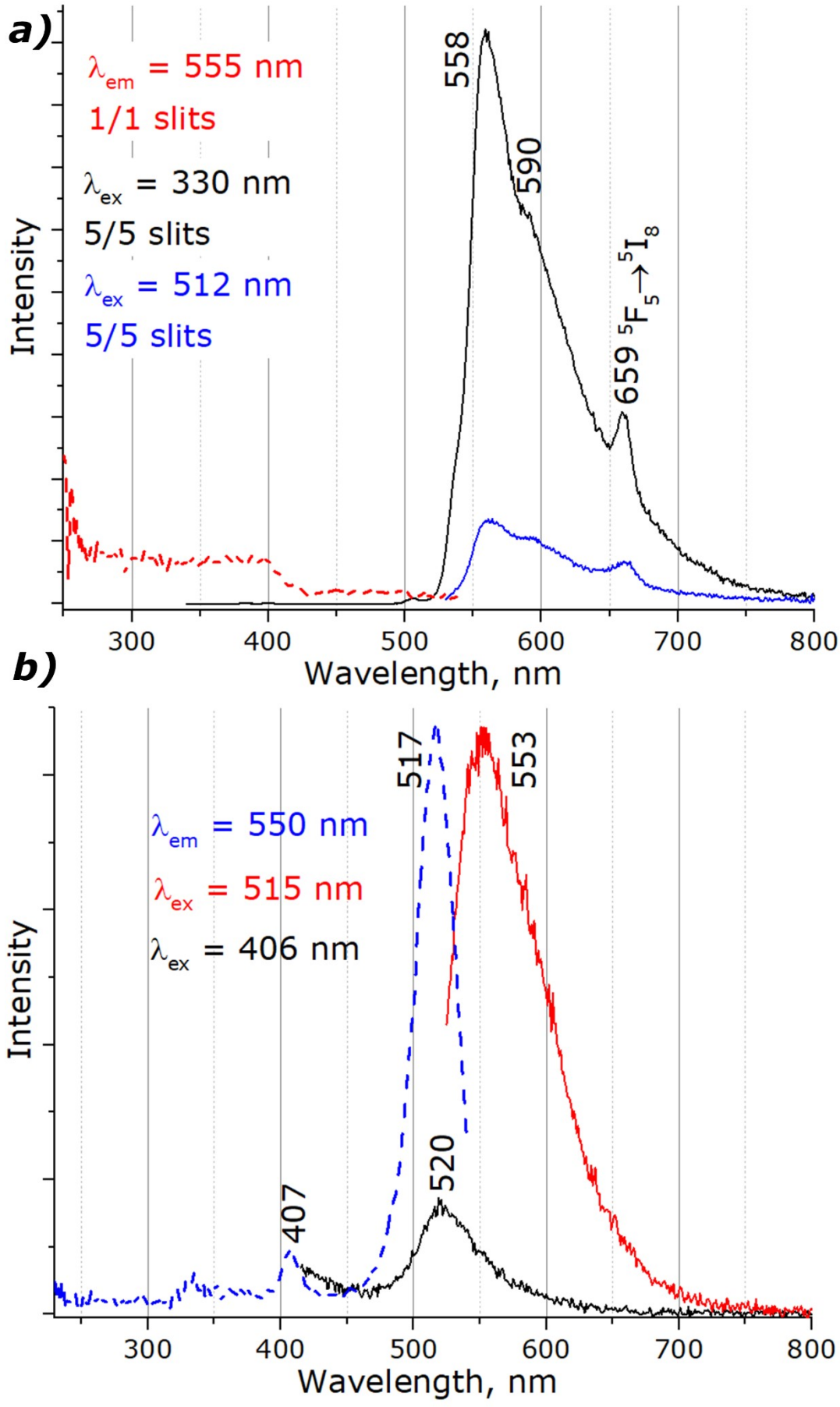

Figure S15. Emission of **4**^{Ho} ***a)*** crystalline; ***b)*** in thf solution (C = 1.2 ·10^{-3} M). The excitation plots are shown with dashed lines, the emission plots are shown with solid lines.

6. Structure of Li-NHPbt

A single crystal of $[Li(thf)NHPbt]_2$ was obtained in a very minor amount upon crystallization of **1^H** from toluene containing a residual amount of thf. The dimeric molecule consists of two units {Li(thf)NHPbt} and is centrosymmetric. Li cations form almost planar chelate cycles with a deviation of 0.12 Å from the mean plane (N C1 C2 C2' N3'). Two mean planes of Pbt fragments are symmetrically parallel, they intersect the central plane (N Li N'' Li'') at an 80° angle. Despite Pbt cycles planarity, the parallel π-stacking interactions in the crystalline structure are not observed. However, T-shaped contacts can still be found between a sulfur atom and a neighbor benzothiazole of another molecule.

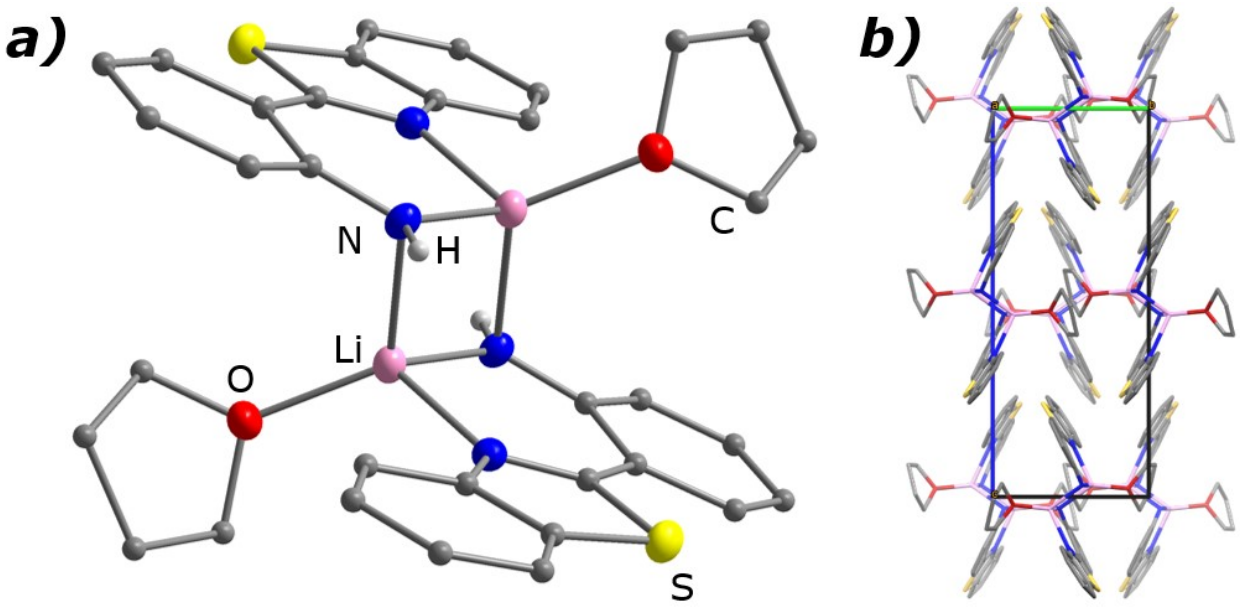

Figure S16. ***a)*** Molecular structure of Li-NHPbt (hydrogen atoms are omitted, non-carbon atoms are represented as 50% probability ellipsoids); ***b)*** packing view along *a* axis in a capped sticks view.